Korea-Australia Rheology Journal
Vol. 18, No. 4, December 2006 pp. 209-215

A review on viscocapillary models of pre-metered coating flows

Suk Il Youn, Su Yeon Kim, Dong Myeong Shin, Joo Sung Lee[1], Hyun Wook Jung* and Jae Chun Hyun
Department of Chemical and Biological Engineering, Applied Rheology Center, Korea Univesity, Seoul 136-713, Korea
[1]Department of Chemical Engineering, University of California at Berkeley, Berkeley, CA 94720, USA
(Received December 12, 2006)

Abstract

Recent research results on viscocapillary models of various pre-metered coating flows such as curtain, slide, and slot coatings have been reviewed in this paper. Such one-dimensional models have been simplified from two-dimensional Navier-Stokes equations for viscous coating flows with free surfaces, using integral momentum balances and lubrication approximation. It has been found that these viscocapillary models is capable of predicting flow dynamics in various coating systems, providing the good agreement with results by 2-D models.

Keywords : Curtain coating, slide coating, slot coating, viscocapillary model, integral momentum balance

1. Introduction

Coating is generally defined as the displacement of air from a solid substrate or web by a coating liquid in order to deposit a continuous or discrete thin layer until it is dried or solidified. Coating processes are indispensable in the manufacture of both commodity and specialty products including flat panel displays, Li-ion batteries, fuel cells, papers, adhesive/magnetic tapes, photographic films, electronic circuit boards, integrated circuits, Cr-free steels, and so on.

There are many varieties of coating processes such as pre-metered types (e.g., curtain, slide, and slot coatings) and self-metered or post-metered types (e.g., roll and blade coatings). In the pre-metered coatings which are mainly focused in this study, the final coating layer thickness is exactly evaluated from the continuity relationship of coating liquids, whereas it depends on coating method itself in the post-metered coatings (Cohen and Gutoff, 1992).

Both theoretical considerations, i.e., flow dynamics in coating bead regions, process stability and sensitivity, and experimental observations with the ingenious flow visualization techniques for these coating processes have been successfully and steadily developed by many researchers (Cohen and Gutoff, 1992; Gutoff and Cohen, 1995; Kistler and Schweizer, 1997). However, there have been many unresolved issues in this area, e.g., viscoelasticity effect on the coating flow, complex dynamics of multiplayer coatings, high precision coating technology, high-speed technology for productivity enhancement, etc.

*Corresponding author: hwjung@grtrkr.korea.ac.kr

The final goal of coating processes is to deposit uniform coating liquid layer on the web or substrate with the specified coating thickness. However, manufacturing uniform coating products is not a trivial task at high-speed operations because various flow instabilities or defects such as leaking, bubbles, ribbing, and rivulets are frequently observed in coating processes. It is no wonder, therefore, that many efforts to elucidate the various aspects of dynamics and coating windows in coating processes have been made both in academia and industry.

The theoretical analysis for pre-metered coating processes has been mainly developed by means of 2-D Navier-Stokes equation for viscous free surface flows (Kistler, 1983; Christodoulou, 1990; Sartor, 1990; Gates, 1999). Such an analysis is so challenging and time-consuming that a simpler, approximate model would be valuable, once its range of validity were known by comparison with fuller theory and with experiment (Jung *et al.*, 2004). In this paper, we would like to briefly review some recent results on flow dynamics in pre-metered coating processes such as curtain, slide, and slot coatings based on the viscocapillary models.

2. Curtain coating flow

Curtain coating is a pre-metered coating process that has been used to manufacture single-layer and, most notably, multiplayer and patch coatings (Fig. 1a). Coating liquids can be delivered by a slot die (slot-fed type), as in the casting of polymer sheet, or by slide die (slide-fed type). The most important feature of this process is that liquid sheet falls freely without any support in curtain flow region

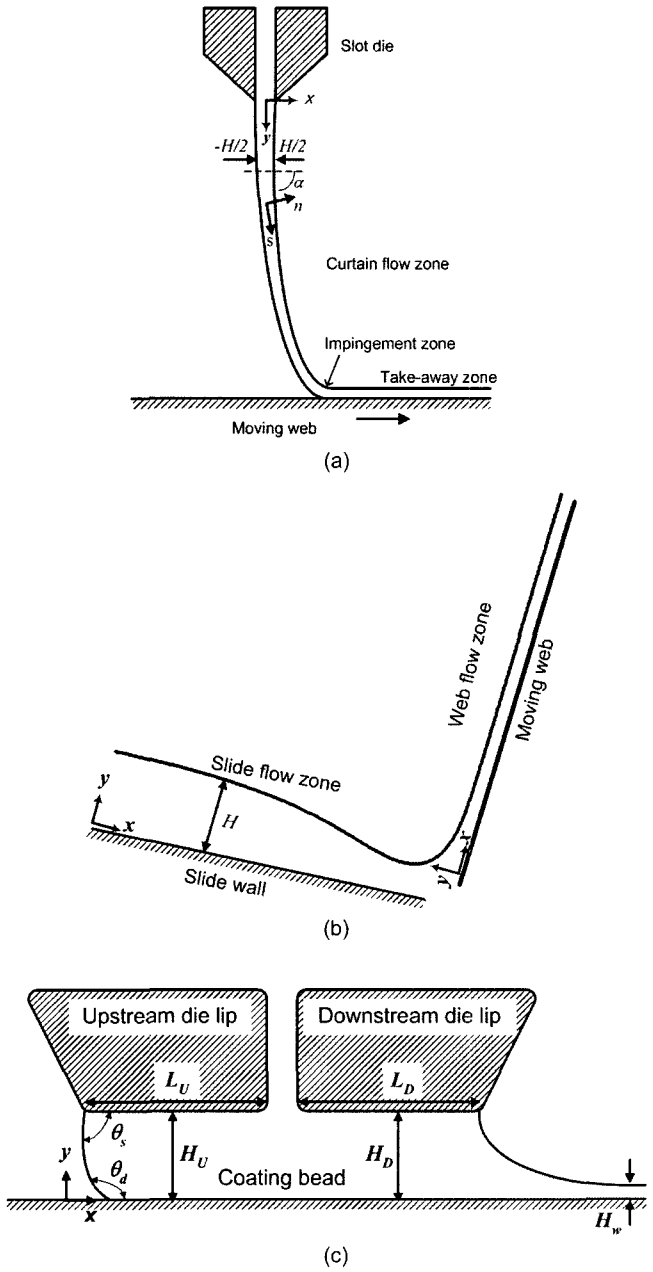

Fig. 1. Schematic diagrams of pre-metered coating processes. (a) Slot-fed curtain coating, (b) slide coating, and (c) slot coating.

before impinging on the substrate being coated and impact pressure at impingement can delay air entrainment up to higher speed.

However, the film or sheet can be very susceptible to unexpected disturbances, e.g., air pressure difference across the curtain (Finnicum *et al.*, 1993; Weinstein *et al.*, 1997), leading to flow instabilities (Jung and Scriven, 2001). Therefore, theoretical modeling is inevitably required to understand, predict, and control curtain behavior.

Curtain coating has been first analysed by Kistler (1983) by means of the 2-D Navier-Stokes governing equations with the free surfaces. This paper has simplified his 2-D equations to viscocapillary ones to simply examine the dynamics of free unsupported liquid curtain, sheet position and trajectory as well as the sheet thickness in curtain flow region.

2-D dimensionless generalized curvilinear Navier-Stokes equations are expressed below (Kistler, 1983).

$$\textit{Equation of continuity:}\ \frac{\partial u}{\partial s}+\frac{\partial (hv)}{\partial n}=0 \tag{1}$$

where, $s=s^*/L$, $n=n^*/T$, $u=u^*T/q$, $v=v^*T/\varepsilon q$, $h=1+\varepsilon\dot{\alpha}n$, $\varepsilon=T/L$

Streamwise equation of motion:

$$Re\left[\frac{\partial u}{\partial \theta}+\frac{1}{h}\left(u\frac{\partial u}{\partial s}+v\frac{\partial}{\partial n}(hu)\right)\right]=-\frac{1}{h}\frac{\partial P}{\partial s}+St\sin\alpha+\frac{1}{h}\frac{\partial \tau_{ss}}{\partial s}$$
$$+\frac{1}{\varepsilon h}\frac{\partial (h\tau_{ns})}{\partial n}+\frac{\tau_{ns}}{h}\dot{\alpha} \tag{2}$$

where, $\theta=t^*q/(TL)$, $\tau=\tau^*TL/(\mu q)$, $P=P^*TL/(\mu q)$ $Re=\rho q/\mu$, $St=\rho gT^2L/(\mu q)$

Crosswise equation of motion:

$$Re\left[\varepsilon\frac{\partial v}{\partial \theta}+\frac{\varepsilon}{h}\left(u\frac{\partial v}{\partial s}+hv\frac{\partial v}{\partial n}\right)\right]-Re\frac{u^2}{h}\dot{\alpha}=-\frac{1}{\varepsilon}\frac{\partial P}{\partial n}-St\cos\alpha+\frac{1}{h}\frac{\partial \tau_{ns}}{\partial s}$$
$$+\frac{1}{\varepsilon h}\frac{\partial (h\tau_{nn})}{\partial n}-\frac{\tau_{ss}}{h}\dot{\alpha} \tag{3}$$

Extra stress components:

$$\tau_{ss}=2\left(\frac{1}{h}\frac{\partial u}{\partial s}+\frac{v}{h}\frac{\partial h}{\partial n}\right),\ \tau_{nn}=2\frac{\partial v}{\partial n},\ \tau_{ns}=\varepsilon\frac{1}{h}\frac{\partial v}{\partial s}+\frac{h}{\varepsilon}\frac{\partial}{\partial n}\left(\frac{u}{h}\right) \tag{4}$$

where, θ denotes the dimensionless time, s the dimensionless streamwise direction, n the dimensionless crosswise direction, h the scale factor, ε the aspect ratio of curtain thickness to flow distance, u the dimensionless streamwise velocity component, v the dimensionless crosswise velocity component, τ_{ij} the dimensionless extra stress components, μ Newtonian viscosity, P the dimensionless isotropic pressure, α the inclination angle of mid-surface from the horizontal line, T the characteristic curtain thickness, L the characteristic flow length, q the flow rate per curtain width, Re Reynolds number, and St Stokes number. Overdot means the derivatives with respect to s and superscript asterisk denotes dimensional properties. The following boundary conditions are incorporated within above governing equations to completely solve the free surface systems.

Normal stress condition at free surfaces:

$$-P_{\pm}^{B}+P_{\pm}^{A}+\frac{1}{Ca}2\kappa_{\pm}+\tau_{nn\pm}\mp\varepsilon\left(\frac{\dot{H}}{2}\right)\frac{1}{h}\tau_{ns\pm}=0 \quad \text{at} \quad n=\pm\frac{H}{2} \tag{5}$$

where $\kappa_{\pm}=\dot{\alpha}(s)$, $Ca=\mu q'/(\sigma T)$

Tangential stress condition at free surfaces:

$$-\varepsilon^2 h_{\pm}\left(\frac{\dot{H}}{2}\right)(\tau_{ss}-\tau_{nn})_{\pm}+\varepsilon\left[\pm h_{\pm}^2\mp\varepsilon^2\left(\frac{\dot{H}}{2}\right)^2\right]\tau_{ns\pm}=0 \quad \text{at} \quad n=\pm\frac{H}{2} \tag{6}$$

Kinematic condition at free surfaces:

$$u_{\pm}=\frac{\pm h_{\pm}}{(\dot{H}/2)}\left(v_{\pm}\mp\frac{\partial}{\partial t}\left(\frac{H}{2}\right)\right) \quad \text{at} \quad n=\pm\frac{H}{2} \tag{7}$$

where $\kappa_{\pm}$ represents the curvature of free surface, Ca capillary number, σ surface tension, H the curtain thickness, superscripts A and B the air and liquid phases, and subscripts + and – are the right and left free surfaces, respectively.

Next step is to integrate both streamwise and crosswise equations of motion (Eqs. 2~3) over sheet thickness from $-H/2$ to $H/2$, incorporating with the free surface boundary conditions, as given in Eqs. 8~9.

Integrated streamwise equation of motion:

$$\begin{aligned}&Re\frac{\partial}{\partial\theta}\int_{-H/2}^{H/2}hu\,dn-\varepsilon Re\frac{\partial\dot{\alpha}}{\partial\theta}\int_{-H/2}^{H/2}un\,dn+\frac{\partial}{\partial s}\int_{-H/2}^{H/2}(Reu^2-\tau_{ss})dn\\&+\dot{\alpha}\int_{-H/2}^{H/2}(\varepsilon Reuv-\tau_{ns})dn+\frac{\partial}{\partial s}\int_{-H/2}^{H/2}p\,dn\\&-\left(\frac{\dot{H}}{2}\right)\left(P_+^A+\frac{1}{Ca}2k_++P_-^A+\frac{1}{Ca}2k_-\right)-HSt\sin\alpha=0\end{aligned} \tag{8}$$

Integrated crosswise equation of motion:

$$\begin{aligned}&\varepsilon Re\frac{\partial}{\partial\theta}\int_{-H/2}^{H/2}hv\,dn-\varepsilon^2Re\frac{\partial\dot{\alpha}}{\partial\theta}\int_{-H/2}^{H/2}vn\,dn+\frac{\partial}{\partial s}\int_{-H/2}^{H/2}(\varepsilon Reuv-\tau_{ns})dn\\&-\dot{\alpha}\int_{-H/2}^{H/2}(Reu^2-\tau_{ss})dn=\frac{-h_+}{\varepsilon}\left(P_+^A+\frac{1}{Ca}2k_+\right)+\frac{h_-}{\varepsilon}\left(P_-^A+\frac{1}{Ca}2k_-\right)\\&+\dot{\alpha}\int_{-H/2}^{H/2}P\,dn-HSt\cos\alpha\end{aligned} \tag{9}$$

It is the core to eliminate the pressure distribution in the above integrated equations of motion using the following pressure equality relation.

$$2P(n)=P(H/2)+P(-H/2)+\int_{H/2}^{n}\frac{\partial P}{\partial n}dn+\int_{-H/2}^{n}\frac{\partial P}{\partial n}dn \tag{10}$$

Inserting normal stress boundary condition and crosswise equation of motion in Eq. (10), yields pressure distribution, $P(n)$.

$$\begin{aligned}P(n)=&\frac{1}{2}\left[P_+^A+P_-^A+\frac{1}{Ca}2k_++\frac{1}{Ca}2k_-\right]\\&-n\varepsilon St\cos\alpha+\tau_{nn}-\varepsilon^2Rev^2+\phi\end{aligned} \tag{11}$$

where

$$\begin{aligned}\phi=&-\frac{1}{2}\dot{\alpha}\left[\int_{H/2}^{n}\frac{1}{h}[\varepsilon Re(u^2-\varepsilon^2v^2)+\varepsilon(\tau_{nn}-\tau_{ss})]dn\right.\\&\left.+\int_{-H/2}^{n}\frac{1}{h}[\varepsilon Re(u^2-\varepsilon^2v^2)+\varepsilon(\tau_{nn}-\tau_{ss})]dn\right]\\&+\frac{1}{2}\frac{\partial}{\partial s}\left[\int_{H/2}^{n}\frac{1}{h}[\varepsilon^2Reuv-\varepsilon\tau_{ns}]dn+\int_{-H/2}^{n}\frac{1}{h}[\varepsilon^2Reuv-\varepsilon\tau_{ns}]dn\right]\\&+\frac{1}{2}\varepsilon^2\ddot{\alpha}\left[\int_{H/2}^{n}\frac{n}{h}[\varepsilon Reuv-\tau_{ns}]dn+\int_{-H/2}^{n}\frac{n}{h}[\varepsilon Reuv-\tau_{ns}]dn\right]\\&+\frac{1}{2}\varepsilon^2Re\frac{\partial}{\partial\theta}\left[\int_{H/2}^{n}v\,dn+\int_{-H/2}^{n}v\,dn\right]\end{aligned}$$

Exact integrodifferential equations of motion are finally obtained when Eq. (11) is substituted into the integrated pressure terms of Eqs. 8~9 as follows.

Integrodifferential streamwise equation of motion:

$$\begin{aligned}&Re\frac{\partial}{\partial\theta}\int_{-H/2}^{H/2}hu\,dn-\varepsilon Re\frac{\partial\dot{\alpha}}{\partial\theta}\int_{-H/2}^{H/2}un\,dn\\&+\frac{\partial}{\partial s}\int_{-H/2}^{H/2}[(Reu^2-\varepsilon^2Rev^2)+(\tau_{nn}-\tau_{ss})]dn\\&+\dot{\alpha}\int_{-H/2}^{H/2}(\varepsilon Reuv-\tau_{ns})dn-HSt\sin\alpha\\&+\left(\frac{H}{2}\right)\frac{\partial}{\partial s}\left(P_+^A+P_-^A+\frac{1}{Ca}2k_++\frac{1}{Ca}2k_-\right)+\frac{\partial}{\partial s}\int_{-H/2}^{H/2}\phi\,dn=0\end{aligned} \tag{12}$$

Integrodifferential crosswise equation of motion:

$$\begin{aligned}&\varepsilon Re\frac{\partial}{\partial\theta}\int_{-H/2}^{H/2}hv\,dn-\varepsilon^2Re\frac{\partial\dot{\alpha}}{\partial\theta}\int_{-H/2}^{H/2}vn\,dn+\frac{\partial}{\partial s}\int_{-H/2}^{H/2}(\varepsilon Reuv-\tau_{ns})dn\\&-\dot{\alpha}\int_{-H/2}^{H/2}[(Reu^2-\varepsilon^2Rev^2)+(\tau_{nn}-\tau_{ss})]dn+\frac{1}{\varepsilon}(P_+^A-P_-^A)\\&+\frac{1}{\varepsilon Ca}(2k_+-2k_-)+HSt\cos\alpha-\dot{\alpha}\int_{-H/2}^{H/2}\phi\,dn=0\end{aligned} \tag{13}$$

Also, equation of continuity including time dependent term (Eq. 14) can be easily derived by integrating equation of continuity over the curtain thickness coupled with the kinematic free surface boundary condition.

$$\frac{\partial H}{\partial t}+\frac{\partial}{\partial s}(uH)=0 \tag{14}$$

Finally, viscocapillary equations comprising the equation of continuity, two equations of motion are simplified by the several assumptions that curtain sheet thickness is very small compared to the length scale of flow direction, i.e., "thin sheet approximation," (very small ε) and shear stress is neglected in the curtain flow because this region is mainly governed by uniaxial extensional flow like polymer extensional deformation processes, e.g., fiber spinning and film casting, and deformation and velocity component normal to curtain trajectory are also negligible. The 1-D viscocapillary equations are represented below.

Simplified equation of continuity:

$$\frac{\partial H}{\partial \theta}+[\sin\alpha]\frac{\partial}{\partial y}(uH)=0 \tag{15}$$

Simplified streamwise equation of motion:

$$ReH\frac{\partial u}{\partial \theta}+ReuH\sin\alpha\frac{\partial u}{\partial y}-4\sin\alpha\frac{\partial}{\partial y}\left(\sin\alpha\frac{\partial u}{\partial y}H\right)-HSt\sin\alpha=0 \tag{16}$$

Simplified crosswise equation of motion:

$$-[\sin\alpha]\frac{\partial\alpha}{\partial y}Reu^2H+4[\sin^2\alpha]\frac{\partial\alpha}{\partial y}\frac{\partial u}{\partial y}H+\Delta P+\frac{2}{Ca}\sin\alpha\frac{\partial\alpha}{\partial y}+HSt\cos\alpha=0 \tag{17}$$

where ΔP is the air pressure difference across the curtain and y the vertical height from the die exit to web position. Streamwise equation of motion balances streamwise inertia, viscous tensile, and streamwise gravity. Crosswise equation of motion balances crosswise inertia, viscous tensile, air pressure difference across the curtain, capillary force, and crosswise gravity.

One interesting point is that viscocapillary model includes air pressure difference across the curtain in the streamwise equation of motion. Air pressure difference may be important because the liquid curtain gives rise to high impact pressure at the impingement region (Finnicum *et al.*, 1993). It is confirmed that if the curtain falls vertically under zero air pressure difference condition, above equations coincide with those by Brown (1961) and Kistler (1983).

One example of steady curtain trajectories in curtain flow region, depending on the process conditions, is depicted in Fig. 2. As Re increases, curtain is deflected back and forth, qualitatively agreeing with 2-D simulation results by Kistler (1983). More detailed results on stability and frequency response in 1-D slot-fed curtain flow will be reported later by the authors (Youn *et al.*, 2007).

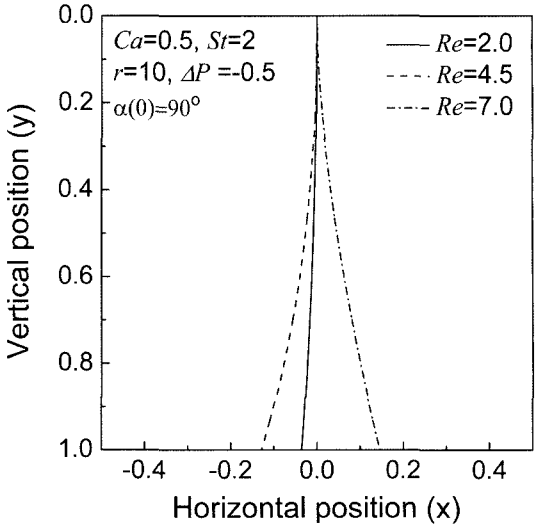

Fig. 2. Curtain deflection in curtain coating process when *Re* increases.

3. Slide coating flow

Slide coating process basically includes a slide die with an inclined plane, placed at a small distance (0.2 to 0.4 mm) from a moving web. One of advantages of this process is to produce multilayer film widely used in photographic industry. Although there are many important theoretical issues in this process (Christodoulou, 1990; Kistler and Schweizer, 1997), viscocapillary model and its steady results have only been focused in this section. Derivation of viscocapillary models for flow dynamics in the slide wall and moving web regimes is similar to the curtain coating case, using the integral momentum balances of Navier-Stokes equation (Nagashima, 2004; Jung *et al.*, 2004). The exemplary viscocapillary equations for predicting the steady sheet thickness profiles are shown below in the slide coating (The detailed derivation of viscocapillary model and boundary conditions is referred to Nagashima, 2004 and Jung *et al.*, 2004).

Flow model on the inclined plane:

$$\frac{d\kappa}{dx}=Ca\left(-\frac{6Re}{5H^3}+St\sin\theta\right)\frac{dH}{dx}+\frac{3Ca}{H^3}-Ca\,St\cos\theta \tag{18}$$

where $\kappa=\dfrac{d^2H/dx^2}{(1+(dH/dx)^2)^{3/2}}$

Flow model on the web:

$$\frac{d\kappa}{dx}=Ca\left(\frac{Re}{5}\left(\frac{U_w^2}{H}-\frac{6}{H^3}\right)+St\sin\phi\right)\frac{dH}{dx}+Ca\left(\frac{3}{H^3}-\frac{3U_w}{H^2}\right)+Ca(St\cos\phi) \tag{19}$$

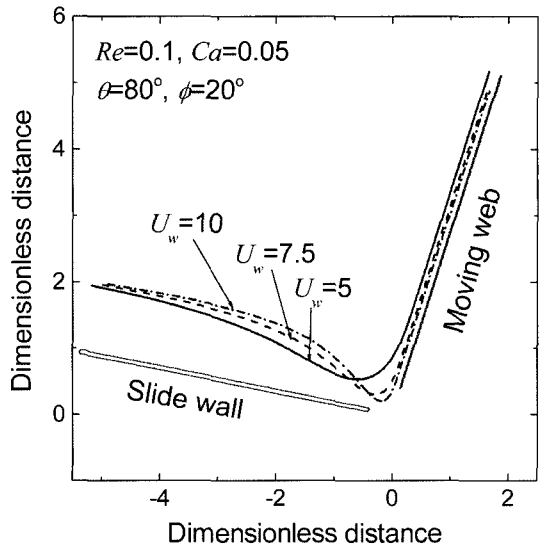

Fig. 3. Effect of web speed on the sheet thickness in slide coating process.

where H denotes the dimensionless sheet thickness, x the flow direction coordinate, θ the inclination angle of slide wall, ϕ the inclination angle of moving web, κ curvature, and U_w the dimensionless web velocity.

Fig. 3 displays the effect of web speed on the slide coating flow determined by the viscocapillary model. It is clearly seen that the web speed makes the standing wave in inclined slide larger.

4. Slot coating flow

In slot coating, coating liquids issuing from feed slot are coated on the surface of moving web typically operated at high speeds after passing through the coating bead region which is the liquid span between the upstream and downstream die lips and the web. A slight vacuum can be applied at the upstream meniscus region for the stabilization of the coating bead (Sartor, 1990; Kistler and Schweizer, 1997; Gates, 1999).

As in the other coating methods, slot coating process should be carefully controlled to prevent coating defects that mar the uniformity of the coating layer, e.g., leaking, air bubbles, barring, ribbing, rivulets, etc. (Gates, 1999; Carvalho and Kheshgi, 2000). The occurrence of these instabilities critically depends on design (e.g., upstream/downstream lips, gap size between die and web, and slot gap), operating (e.g., flow rate, web speed, and bead pressure), and physical parameters (e.g., viscosity, density, viscoelasticity, and surface tension) in this process. For example, leaking occurs when the upstream meniscus has maximum curvature at the upstream edge of the upstream lip, breaking the pre-metered condition and bead break-up phenomena including ribbing, rivulet, air entrainment, and barring happen as the upstream meniscus reaches its maximum curvature at the downstream edge of the upstream lip. Therefore, it is essential to understand the flow behavior inside the coating bead and establish the optimal operability coating windows for the uniform coating in slot coating, depending on process conditions.

Simplified 1-D viscocapillary model to predict the steady flows in coating bead can be derived by assuming the rectilinear flow in that region (Ruschak, 1976; Higgins and Scriven, 1980). Flows in both upstream and downstream gaps can be predicted by the combination of the Couette flow caused by the moving web and the Poiseuille flow by pressure drop for the sake of the continuity condition. First, the equation of motion in coating bead region is simply reduced, as shown in Eq. (20), assuming that inertia and gravity forces are relatively small compared with viscous and capillary forces.

$$-\frac{\partial P}{\partial x}+\mu\left(\frac{\partial^2 u}{\partial y^2}\right)=0 \tag{20}$$

This simple equation is subjected to the following boundary conditions.

$$u=U_w \text{ at } y=0 \tag{21a}$$
$$u=0 \text{ at } y=H_i \tag{21b}$$

where μ represents Newtonian viscosity, P the isotropic pressure, U_w the web speed, H_i (H_U and H_D) the coating gap sizes at upstream and downstream regions, and x and y the flow direction and normal direction coordinates, respectively. The net flow in the upstream region of the coating bead is actually zero, whereas that in the downstream region is the flux of coating liquid carried by moving web.

$$q_U=-\frac{H_U^3}{12\mu}\left(\frac{P_f-P_U^L}{x_f-x_U}\right)+\frac{U_w}{2}H_U=0 \tag{22}$$

$$q_D=-\frac{H_D^3}{12\mu}\left(\frac{P_D^L-P_f}{x_D-x_f}\right)+\frac{U_w}{2}H_D=U_wH_w \tag{23}$$

Here q_U and q_D denote the flow rates per the width at upstream and downstream regions, P_f the pressure at feed slot, P_U^L and P_D^L the pressures in the liquid phase at the upstream and downstream menisci, and H_w the final coating thickness.

Using the Young-Laplace equation relating the pressure in the gas phase to that in the liquid phase, P_U^L and P_D^L are substituted with pressures in gas phase, i.e., P_U and P_D. Regarding the upstream meniscus shape as an arc-of-circle that meets the upstream lip with static contact angle, θ_s, and the web with dynamic contact angle, θ_d (Higgins and Scriven, 1980), incorporating the Landau-Levich film flow approximation for downstream meniscus shape (Middleman, 1977), and finally combining Eqs. 22~23 to eliminate feed pressure, P_f, 1-D viscocapillary model has been derived

(Gates, 1999).

$$l_U = x_f - x_U = \frac{H_U^2}{6\mu U_w}\left(\Delta P - 1.34Ca^{2/3}\frac{\sigma}{H_w} + \frac{\sigma}{H_U}(\cos\theta_s + \cos\theta_d)\right)$$

$$-\frac{H_U^2}{H_D^2}\left(1-2\frac{H_w}{H_D}\right)L_D \qquad (24)$$

where l_U denotes the length of the upstream bead, x_U the upstream meniscus position, x_f the feed position, ΔP the bead pressure drop (the difference between ambient pressures acting on upstream and downstream menisci), L_D the downstream die lip length. It is possible to approximately establish coating limits (leaking and bead break-up) by calculating the upstream meniscus location under various process conditions.

Coating limits determined from the position of upstream meniscus using Eq. (24) are obtained in the form of bead pressure drop and web speed (Fig. 4) and also compared with those from 2-D CFD software, Flow-3D under the same process conditions. Leaking defect that the coating liquid issues into vacuum box occurs under high bead pressure drop or low web speed conditions and bead break-up is generated at low bead pressure drop or high web speed. This figure also demonstrates the good agreement of results by 1-D and 2-D simulations.

Interestingly, using the transient 1-D model, sensitivity analysis (frequency response in this study) of this process has been performed. By introducing the sinusoidal ongoing disturbances at flow rate, web speed, bead pressure, and upstream/downstream gaps, sinusoidal changes and amplitudes of final wet film thickness have been evaluated.

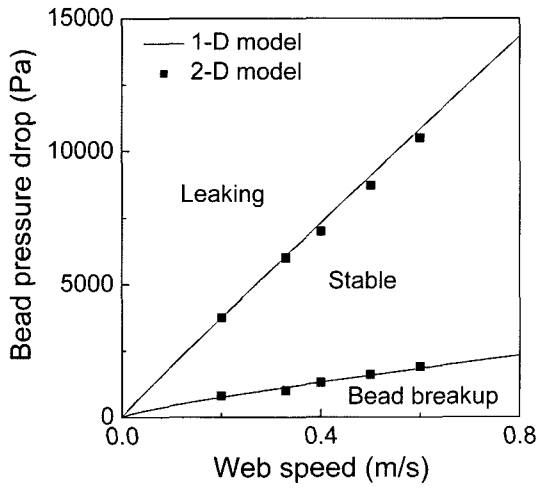

Fig. 4. Example of stability windows in the form of bead pressure vs. web speed in slot coating. (Lines denote results by 1-D model and symbols represent those by 2-D model. $H_U = H_D = 200$ μm, $\sigma = 67$ mN/m, $\mu = 36$ cP, $L_U = L_D = 1000$ μm, $H_w = 90$ μm, $\theta_s = 60°$, $\theta_d = 120°$).

To analyze the sensitivity response of wet film thickness with respect to unexpected disturbances or perturbations, frequency response analysis has been conducted (Gates, 1999; Kim *et al.*, 2005). Fig. 5(a) shows the sinusoidal change of wet film thickness when the ongoing disturbance with 5% amplitude is introduced in web speed. As the oscillating frequency of the disturbance increases, the sensitivity of film thickness gets lower. Fig. 5(b) exhibits the whole sensitivity of wet film thickness with respect to various disturbances. It is noted that the ongoing gap disturbance with high frequency makes the system more sensitive. Systematic analyses of the effect of die geometry

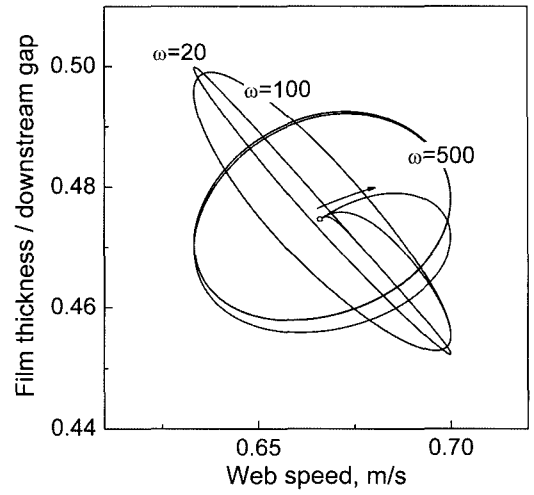

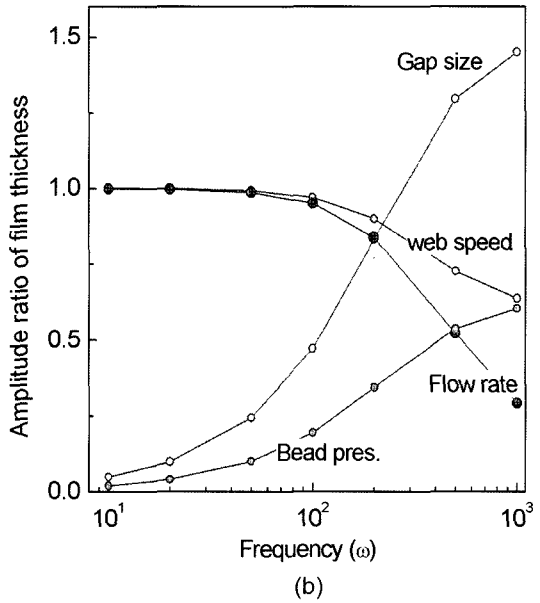

Fig. 5. (a) Sinusoidal change of wet film thickness with respect to ongoing disturbance with 5% amplitude at web speed and (b) amplitude ratio between wet film thickness and various input disturbances.

and process conditions on the slot coating dynamics then make possible further stabilization and optimization strategies to improve the process productivity.

Acknowledgements

This study was supported by research grants from Seoul R&BD Program and the Korea Science and Engineering Foundation (KOSEF) through the Applied Rheology Center (ARC), Seoul, Korea.

References

Brown, D.R., 1961, A study of the behavior of a thin sheet of moving liquid, *J. Fluid Mech.* **10**, 297-305.

Carvalho, M.S. and H.S. Kheshgi, 2000, Low-flow limit in slot coating: Theory and experiment, *AIChE J.* **46**, 1907-1917.

Christodoulou, K.N., 1990, Computational Physics of Slide Coating Flow, PhD Thesis, University of Minnesota.

Cohen, E.D. and E.B. Gutoff, 1992, Modern Coating and Drying Technology, VCH Publishers, New York.

Finnicum, D.S., S.J. Weinstein and K.J. Ruschak, 1993, The effect of applied pressure on the shape of a two-dimensional liquid curtain falling under the influence of gravity, *J. Fluid Mech.* **255**, 647-665.

Gates, I.A., 1999, Slot Coating Flows: Feasibility, Quality. PhD Thesis, University of Minnesota.

Gutoff, E.B. and E. D. Cohen, 1995, Coating and Drying Defects, John Wiley & Sons, New York.

Higgins, B.G. and L.E. Scriven, 1980, Capillary-pressure and viscous pressure-drop set bounds on coating bead operability, *Chem. Eng. Sci.* **35**, 673-682.

Jung, H.W. and L.E. Scriven, 2001, Simplified modeling of curtain coating, *AIChE National Meeting*, Reno, Nevada, USA.

Jung, H.W., J.S. Lee, J.C. Hyun, S.J. Kim and L.E. Scriven, 2004, Simplified modelling of slide-fed curtain coating flow, *Korea-Australia Rheology J.* **16**, 227-233.

Kim, S.Y., W.S. Park, H.W. Jung, M.-S. Park and D.-H. Shin, 2005, Dynamics and operability windows of slot coating process, The 6th European Coating Symposium, Bradford, UK.

Kistler, S.F., 1983, The Fluid Mechanics of Curtain Coating and Related Viscous Free Surface Flows with Contact Lines, PhD Thesis, University of Minnesota.

Kistler, S.F. and P.M. Schweizer, 1997, Liquid Film Coating, Chapman & Hall, London.

Middleman, S., 1977, Fundamentals of Polymer Processing, McGraw-Hill, New York.

Nagashima, K., 2004, Viscocapillary modeling of slide coating flow, *Industrial Coating Research* **5**, 81-106.

Ruschak, K.J., 1976, Limiting flows in a pre-metered coating device, *Chem. Eng. Sci.* **31**, 1057-1060.

Sartor, L., 1990, Slot Coating: Fluid Mechanics and Die Design, PhD Thesis, University of Minnesota.

Weinstein, S.J., A. Clarke and E.A. Simister, 1997, Time-dependent equations governing the shape of a two-dimensional liquid curtain, Part 1: Theory, *Phys. Fluids* **9**, 3625-3636.

Youn, S.I., D.M. Shin, J.S. Lee, H.W. Jung and J.C. Hyun, 2007, Stability and sensitivity of curtain coating process using viscocapillary model, In preparation.